Riemannian geometric approach to human arm dynamics, movement optimization, and invariance

Armin Biess*
Bernstein Center for Computational Neuroscience, DE-37073 Göttingen, Germany and
Max-Planck-Institute for Dynamics and Self-Organization, DE-37073 Göttingen, Germany

Tamar Flash
Department of Applied Mathematics and Computer Science, The Weizmann Institute of Science, Rehovot IL-76100, Israel

Dario G. Liebermann
Physical Therapy Department, Sackler Faculty of Medicine, Tel Aviv University, Ramat Aviv IL-69978, Israel
(Received 9 September 2010; published 31 March 2011)

We present a generally covariant formulation of human arm dynamics and optimization principles in Riemannian configuration space. We extend the one-parameter family of mean-squared-derivative (MSD) cost functionals from Euclidean to Riemannian space, and we show that they are mathematically identical to the corresponding dynamic costs when formulated in a Riemannian space equipped with the kinetic energy metric. In particular, we derive the equivalence of the minimum-jerk and minimum-torque change models in this metric space. Solutions of the one-parameter family of MSD variational problems in Riemannian space are given by (reparametrized) geodesic paths, which correspond to movements with least muscular effort. Finally, movement invariants are derived from symmetries of the Riemannian manifold. We argue that the geometrical structure imposed on the arm's configuration space may provide insights into the emerging properties of the movements generated by the motor system.

DOI: 10.1103/PhysRevE.83.031927 PACS number(s): 87.19.rs, 45.10.Na, 02.40.Ky, 87.19.lr

I. INTRODUCTION

The computational principles underlying the generation of voluntary human motor actions are still largely unknown. Reaching for an object, for example, requires multiple sensorimotor transformations from visual to motor space. It has been suggested that this process can be regarded as a mapping problem between different sensorimotor spaces, such as the transformation from retinal coordinates of visual space into movement trajectories of task space and eventually joint angular coordinates of arm configuration space [1,2]. Interestingly, Mach and Poincaré [3,4] have pointed out more than a century ago the fundamental differences between sensory spaces and Euclidean space with regard to continuity, dimensionality, spatial extension, homogeneity, and isotropy. Which underlying geometrical structure do sensorimotor spaces have? Perceptual space, for example, has been investigated most extensively and different non-Euclidean geometric structures have been proposed to describe it, ranging from Riemannian manifolds with varying curvature [5,6] to nonmetric spaces with affine or projective geometry [7,8].

We mention briefly a few approaches that tried to incorporate geometrical methods into sensorimotor control. Pellioniz and Llinás have proposed a "tensor network theory of the cerebellum," where a covariant sensory vector is transformed into a contravariant motor execution vector by the cerebellum, which acts as a metric tensor of a non-Euclidean neural space [1]. Although this approach promotes a description of sensorimotor control as a remapping problem, it has some theoretical flaws. For example, it neither provides a mathematical definition of the neural manifold under consideration nor does it specify its metric structure [2]. Hestenes has formulated a neurogeometry of sensorimotor control using geometric algebra. Based on the assumption that motor neuron signals encode solely kinematic states, a coordinate-free formulation of eye-head kinematics [9] and body kinematics [10] is provided. A differential geometric approach using Lie groups and affine geometry to model eye and arm movements has also been used [11,12].

In this paper, we model the space of arm configurations as a Riemannian manifold and show that this geometric approach leads to a unification of existing computational models of human arm movements between pointlike targets. It is proposed that point-to-point movements along geodesic paths in the configuration manifold emerge from properties of the motor system, which intends to reduce muscular effort. Whereas Riemannian geometry has been extensively applied in mechanics, particularly in robotics, it has found little expression in formulations within models of human motor control [12–16]. The main objective of the Riemannian formulation lies in the determination of a suitable metric that is meaningful to the problem under consideration. Once a metric structure is identified, a Riemannian model formulation is appealing for several reasons. First, expressions can be written in a coordinate-independent or generally covariant form. Second, the Riemannian formulation facilitates the identification of intrinsic relations and encompasses the transformation rules between different sets of coordinates. Third, movement invariants can be derived from symmetries of the underlying Riemannian space. Note that invariant movement features are assumed to be a by-product of constraints imposed by the brain to enable control of a multiple degrees of freedom system. Thus, this paper elaborates on a differential geometric formulation of models in human motor control.

*Corresponding author: armin@nld.ds.mpg.de

In a previous paper, we have assumed that the movement properties can be derived by applying separate optimization principles on the temporal and spatial levels of control [13]. The spatial characteristics of the movement were determined by geodesic paths in the arm configuration space, whereas the temporal properties followed from the minimization of squared jerk along the hand path. We referred to this model as the geodesic model. We show here, by expressing movement dynamics and optimization principles in a generally covariant form, that the geodesic model can be derived from a one-parameter family of variational problems on the Riemannian manifold. Hence, both the temporal and spatial characteristics of the movements are dictated by the optimization of a single cost in Riemannian space.

Many existing computational models have assumed that human arm movements are planned and optimized by the central nervous system (CNS) prior to movement execution. Accordingly, it has been suggested that movement properties can be derived from integral principles [17–19], similar to action principles in physics. Whereas these formulations resulted in deterministic models, a more recent modeling approach to sensorimotor integration and human motor control is based on stochastic optimal control theory. In this approach, the expectation value of an integral cost is minimized subject to a dynamic constraint given by the equation of motion, including noise [20–22]. This method allows also the incorporation of feedback mechanisms and sensory noise. Despite the merits of a stochastic formulation, in this paper we focus on the mean behavior during point-to-point movements and we, therefore, apply a deterministic modeling approach. We remark that both the stochastic and the deterministic approaches require the specification of suitable performance indices, and we will propose in this paper a class of cost functions that correspond to least-effort movements.

Two classical, but fundamentally different, deterministic models have been suggested, namely, the minimum-jerk model (MJ) and the minimum-torque-change (MTC) model. The MJ model is formulated in terms of Cartesian hand position coordinates $\boldsymbol{x}$ and is based on a kinematic cost function that minimizes the squared time derivative of the hand acceleration $\boldsymbol{a} = \ddot{\boldsymbol{x}}$ or jerk integrated over the total movement duration T, i.e.,

$$\delta C_{\mathrm{MJ}} = 0, \quad C_{\mathrm{MJ}} = \int_0^T \langle \dot{\boldsymbol{a}}(t), \dot{\boldsymbol{a}}(t) \rangle_I \, dt, \tag{1}$$

where $\langle \ldots, \ldots \rangle_I$ is the inner product with respect to the Euclidean metric $I = \mathrm{diag}(1,1)$.

In contrast, the MTC model takes movement dynamics into account and postulates a cost function based on the Euclidean inner product of joint torques $\boldsymbol{n}$ integrated over the movement time T:

$$\delta C_{\mathrm{MTC}} = 0, \quad C_{\mathrm{MTC}} = \int_0^T \langle \dot{\boldsymbol{n}}(t), \dot{\boldsymbol{n}}(t) \rangle_I \, dt. \tag{2}$$

The joint torques are determined by the dynamic equation of motion, which is commonly written in vector notation as

$$M(\boldsymbol{q})\ddot{\boldsymbol{q}} + C(\boldsymbol{q},\dot{\boldsymbol{q}})\dot{\boldsymbol{q}} + B(\boldsymbol{q})\dot{\boldsymbol{q}} + \boldsymbol{g}(\boldsymbol{q}) = \boldsymbol{n}(\boldsymbol{q},\dot{\boldsymbol{q}}), \tag{3}$$

where M is the inertia matrix, C is the Coriolis matrix, B is the viscous friction matrix, $\boldsymbol{g}$ denotes the gravitational torques, and $\boldsymbol{q}$ is the vector of joint angles [23]. The components of the Coriolis matrix are defined by $C_{\mu\nu} = \Gamma_{\mu\nu\lambda}\dot{q}^{\lambda}$, where the Christoffel symbols of the first kind follow from the inertia matrix according to

$$\Gamma_{\mu\nu\lambda} = \frac{1}{2}\left(\frac{\partial M_{\mu\nu}}{\partial q^{\lambda}} + \frac{\partial M_{\mu\lambda}}{\partial q^{\nu}} - \frac{\partial M_{\nu\lambda}}{\partial q^{\mu}} \right). \tag{4}$$

The summation convention has been used, implying a summation over the same lower and upper Greek indices from 1 to n, where n is the number of degrees of freedom (DOF) of the arm. It should be pointed out that the MTC model assumes the minimization of the Euclidean norm of joint torques, which is not necessarily the appropriate metric to choose when dealing with intrinsic control variables.

Due to the fundamental differences existing between the MJ and the MTC models, a considerable controversy has emerged concerning the validity of these two models with respect to movement optimization and control. In this paper, we show that the MJ and MTC models are mathematically equivalent when expressed in the Riemannian manifold $\mathcal{M} = (Q,g)$, where the arm's configuration space Q can be regarded as an n-dimensional torus $T^n = S^1 \times \ldots \times S^1$, i.e., as the n-tuple direct product of the circle S^1. There are an infinite number of possible metric structures, expressed in terms of the metric tensor $g = (g_{\mu\nu})$, that one can impose on the manifold. We choose a metric tensor that is derived from the kinetic energy of the arm (kinetic energy metric) and, thus, is closely related to the movement dynamics [24].

II. METHODS

A. Covariant formulation of arm dynamics

We model the human arm as a linkage of rigid bodies with four DOF ($n = 4$). Accordingly, an arm configuration can be described by means of four joint angles $\boldsymbol{q} = (\theta,\eta,\zeta,\phi)^T$ that define a set of generalized coordinates. The first three angles determine the rotation around an ideally spherical shoulder joint (elevation θ, azimuth η, torsion ζ), whereas the rotation around the elbow joint is given by the flexion angle (ϕ). We ignore the DOF at the wrist joint.

Another possible set of four generalized coordinates is defined by $\boldsymbol{q}' = (x,y,z,\alpha)^T$, which consists of the hand coordinates $\boldsymbol{x}$ augmented by the swivel angle α that describes the rotation of the arm triangle around the shoulder-hand axis [25] (see Fig. 1).

There exists a one-to-one map between the coordinates $q^{\mu} = (\theta,\eta,\zeta,\phi)$ and $q'^{\mu} = (x,y,z,\alpha)$. The coordinate differentials are related via the transformation matrix $\Lambda = (\Lambda^{\mu}_{\nu})$:

$$dq'^{\mu} = \Lambda^{\mu}_{\nu}(q)dq^{\nu} \quad \text{with} \quad \Lambda^{\mu}_{\nu} = \frac{\partial q'^{\mu}}{\partial q^{\nu}}. \tag{5}$$

The inverse transformation is $\bar{\Lambda} = \Lambda^{-1}$ and satisfies $\Lambda^{\mu}_{\lambda}\bar{\Lambda}^{\lambda}_{\nu} = \delta^{\mu}_{\nu}$, where δ^{μ}_{ν} is the Kronecker delta. Explicit expression for the one-to-one map between the two sets of coordinates and the transformations Λ of a four and two DOF arm are provided in Appendices A and B, respectively.

There are infinite ways to choose coordinates that are equally well suited for the description of an arm configuration. This ambiguity is addressed by a covariant formulation. The

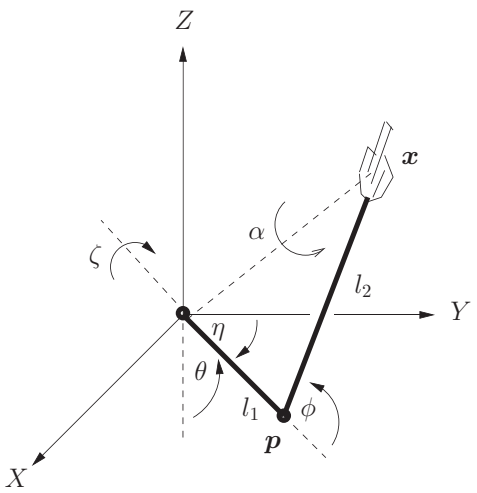

FIG. 1. An arm configuration can be defined by different sets of coordinates, for example, by four joint angular coordinates $q = (\theta,\eta,\zeta,\phi)^T$. Another possible set of generalized coordinates consists of the center of mass of the hand location vector $\boldsymbol{x}$ and the swivel angle α around the shoulder-hand axis, i.e., $q' = (x,y,z,\alpha)^T$. The shoulder joint is fixated and located at the origin of the XYZ coordinate system.

dynamic equation of motion (3) does not have a manifestly covariant form because the second-order derivative of joint angles does not generally transform as a tensor. The covariant form follows from the reformulation of arm dynamics in the Riemannian manifold, which is endowed with the kinetic energy metric [24]. The kinetic energy metric contains the inertial properties of the arm, and its components are determined in the local coordinates q^μ by

$$M_{\mu\nu}(q) = \frac{\partial^2 K(q,\dot{q})}{\partial\dot{q}^\mu\partial\dot{q}^\nu}, \tag{6}$$

where K is the kinetic energy of the arm and $M = (M_{\mu\nu})$. The metric (6) is positive definite and, thus, invertible. The inverse metric is denoted as $M^{\mu\nu} = (M^{-1})_{\mu\nu}$ and satisfies $M^{\mu\lambda}M_{\lambda\nu} = \delta^\mu_\nu$. The Christoffel symbols of the second kind are defined as $\Gamma^\mu_{\nu\lambda} = M^{\mu\rho}\Gamma_{\rho\nu\lambda}$ (see Appendices A and B for explicit expressions of $M_{\mu\nu}$ for a two and four DOF arm). Distances in the arm's configuration space are measured by the line element $d\sigma^2 = M_{\mu\nu}(q)dq^\mu dq^\nu$. Note that the distance measure varies from point to point in the manifold, and is related to the kinetic energy according to $K = 1/2\dot{\sigma}^2$.

We will next define covariant expressions for velocity, acceleration, and jerk in the Riemannian manifold. If $\boldsymbol{V}(t) = \dot{\gamma}(t)$ denotes the velocity along the trajectory $\gamma(t)$, then the acceleration in the Riemannian manifold is given by the covariant derivative along the trajectory $\boldsymbol{A}(t) = \nabla_{\boldsymbol{V}(t)}\boldsymbol{V}(t) \equiv \frac{D\boldsymbol{V}(t)}{dt} \equiv \frac{D^2\gamma(t)}{dt^2}$, where ∇ denotes the Levi-Civita connection on $\mathcal{M} = (T^4, M_{\mu\nu})$, which is the symmetric connection compatible with the metric. The operator $\frac{D}{dt}$ denotes the covariant derivative along the trajectory $\gamma(t)$. Similarly, we can define jerk $\boldsymbol{J}(t) = \frac{D\boldsymbol{A}(t)}{dt} = \frac{D^2\boldsymbol{V}(t)}{dt^2}$ and higher-order time derivatives. Note that the components of the velocity, acceleration, and jerk in the local coordinates q^μ are given by $V^\mu = \dot{q}^\mu$, $A^\mu = \frac{DV^\mu}{dt} = V^\lambda\nabla_\lambda V^\mu = V^\lambda(\partial_\lambda V^\mu + \Gamma^\mu_{\nu\lambda}V^\nu) = \ddot{q}^\mu + \Gamma^\mu_{\nu\lambda}\dot{q}^\nu\dot{q}^\lambda$, and $J^\mu = \dddot{q}^\mu + 3\Gamma^\mu_{\nu\lambda}\ddot{q}^\nu\dot{q}^\lambda + \Gamma^\mu_{\nu\lambda,\rho}\dot{q}^\nu\dot{q}^\lambda\dot{q}^\rho + \Gamma^\mu_{\nu\lambda}\Gamma^\lambda_{\rho\sigma}\dot{q}^\nu\dot{q}^\rho\dot{q}^\sigma$, respectively, and $\boldsymbol{V} = V^\mu\boldsymbol{e}_\mu$, $\boldsymbol{A} = A^\mu\boldsymbol{e}_\mu$, and $\boldsymbol{J} = J^\mu\boldsymbol{e}_\mu$, where $\boldsymbol{e}_\mu = \frac{\partial}{\partial q^\mu}$ denotes the coordinate basis.

We make one further assumption regarding the torques generated by the joints. We assume that the joint torques can be decomposed into configuration-dependent torques $\boldsymbol{\tau}_g$ that compensate for the external gravitational torques and velocity-dependent driving torques $\boldsymbol{\tau}$ that move the arm through space, i.e., we set $\boldsymbol{n}(\boldsymbol{q},\dot{\boldsymbol{q}}) = \boldsymbol{\tau}(\boldsymbol{q},\dot{\boldsymbol{q}}) + \boldsymbol{\tau}_g(\boldsymbol{q})$ with $\boldsymbol{\tau}_g \equiv \boldsymbol{g}$. This assumption, suggested by Atkeson and Hollerbach [26], is based on the idea of the possible separation between torques needed to stabilize the arm against the effect of gravity and those needed for movement generation. We can then rewrite (3) in generally covariant form as

$$M_{\mu\nu}A^\nu = N_\mu, \tag{7}$$

where we have defined $N_\mu \equiv \tau_\mu - B_{\mu\nu}V^\nu$ as the total torque acting on the arm. The friction term is set to zero in the following. Note that the metric tensor maps the covariant acceleration (vector) into the torques (covector). Consider now a coordinate transformation from joint angular coordinates to a new set of coordinates $q^\mu \to q'^\mu$. By multiplying Eq. (7) with $\bar{\Lambda}^T$ and applying the transformation rules (in vector notation) $M' = \bar{\Lambda}^T M\bar{\Lambda}$, $\boldsymbol{A}' = \Lambda\boldsymbol{A}$, and $\boldsymbol{N}' = \bar{\Lambda}^T\boldsymbol{N}$ leaves the form of the dynamic equation in the new coordinates unchanged: $M'_{\mu\nu}A'^\nu = N'_\mu$, i.e., the dynamic equation (7) has a generally covariant form.

III. RESULTS

A. Optimization principles in Riemannian space

We next formulate the MJ in Riemannian space by considering the general class of mean-squared-derivative (MSD) costs of the hand vector $\boldsymbol{x}$, for which the MJ model is a particular member [27]. The MSD models in Euclidean space are described by the one-parameter family of variational problems

$$\delta C_n = 0, \quad C_n = \int_0^T \left\langle \frac{d^n\boldsymbol{x}(t)}{dt^n}, \frac{d^n\boldsymbol{x}(t)}{dt^n} \right\rangle_I dt, \tag{8}$$

where $n = 1,2,\ldots$. Note that, for $n = 3$, the MJ model (1) is recovered.

The generalization of (8) to the Riemannian manifold is straightforward:

$$\delta S_n = 0, \quad S_n = \int_0^T \left\langle \frac{D^{n-1}\boldsymbol{V}(t)}{dt^{n-1}}, \frac{D^{n-1}\boldsymbol{V}(t)}{dt^{n-1}} \right\rangle dt \tag{9}$$

with the definition $\frac{D^0}{dt^0} := 1$. The inner product $\langle\ldots,\ldots\rangle$ is taken with respect to the kinetic energy metric M, i.e., $\langle\boldsymbol{X},\boldsymbol{Y}\rangle = \langle\boldsymbol{e}_\mu,\boldsymbol{e}_\nu\rangle X^\mu Y^\nu = M_{\mu\nu}X^\mu Y^\nu$ for two arbitrary vectors $\boldsymbol{X}$ and $\boldsymbol{Y}$.

The MSD functionals in Riemannian space can be rewritten by repeatedly applying the covariant derivative operator $\frac{D}{dt}$ to the dynamic equation of motion (7). Since the covariant

derivative of the metric tensor vanishes, i.e., $\nabla_\lambda M_{\mu\nu} = 0$, we obtain

$$S_n = \begin{cases} 2\int_0^T K\,dt, & n = 1 \\ \int_0^T \left\langle \frac{D^{n-2}\boldsymbol{\tau}(t)}{dt^{n-2}}, \frac{D^{n-2}\boldsymbol{\tau}(t)}{dt^{n-2}} \right\rangle dt, & n = 2,3\ldots \end{cases} \tag{10}$$

where the case $n = 1$ follows from the definition of the kinetic energy $K = \frac{1}{2}\langle \boldsymbol{V}(t), \boldsymbol{V}(t)\rangle$. In particular, we obtain from (9) and (10) for $n = 1,2,3$ the identities

$$S_1 = \int_0^T \langle \boldsymbol{V}(t), \boldsymbol{V}(t)\rangle dt = 2\int_0^T K(t)dt, \tag{11}$$

$$S_2 = \int_0^T \langle \boldsymbol{A}(t), \boldsymbol{A}(t)\rangle dt = \int_0^T \langle \boldsymbol{\tau}(t), \boldsymbol{\tau}(t)\rangle dt, \tag{12}$$

$$S_3 = \int_0^T \langle \boldsymbol{J}(t), \boldsymbol{J}(t)\rangle dt = \int_0^T \left\langle \frac{D\boldsymbol{\tau}(t)}{dt}, \frac{D\boldsymbol{\tau}(t)}{dt} \right\rangle dt. \tag{13}$$

We remind the reader that the Euclidean expressions of the cost functionals in (11)–(13) have been independently studied in the context of human motor control [17,27,28]. We conclude that the kinematic MSD costs in the Riemannian manifold for $n = 1,2,3$ are identical to the dynamic cost functions defined by the kinetic energy, squared torque, and squared torque change, respectively. In particular, for $n = 3$, we find the equivalence of the MJ and the MTC model in Riemannian space. The Euler-Lagrange equations for the variational problems (11)–(13) follow from the application of the calculus of variation on manifolds [12,29]. We get

$$n = 1\colon \boldsymbol{A} = 0, \tag{14}$$

$$n = 2\colon \frac{D\boldsymbol{J}}{dt} - R(\boldsymbol{V}, \boldsymbol{A})\boldsymbol{V} = 0, \tag{15}$$

$$n = 3\colon \frac{D^3\boldsymbol{J}}{dt^3} - R\left(\boldsymbol{V}, \frac{D\boldsymbol{J}}{dt}\right)\boldsymbol{V} + R(\boldsymbol{A}, \boldsymbol{J})\boldsymbol{V} = 0. \tag{16}$$

For arbitrary $n > 0$, we obtain [30–32]

$$\frac{D^{2n-1}\boldsymbol{V}}{dt^{2n-1}} - \sum_{i=0}^{n-2}(-1)^i R\left(\frac{D^i\boldsymbol{V}}{dt^i}, \frac{D^{2n-3-i}\boldsymbol{V}}{dt^{2n-3-i}}\right)\boldsymbol{V} = 0, \tag{17}$$

where R is the Riemann curvature tensor defined by $R(\boldsymbol{X},\boldsymbol{Y})\boldsymbol{Z} = [\nabla_X, \nabla_Y]\boldsymbol{Z} - \nabla_{[X,Y]}\boldsymbol{Z}$ for arbitrary vector fields $\boldsymbol{X},\boldsymbol{Y},\boldsymbol{Z}$ and $[\ldots,\ldots]$ denotes the commutator [33]. The solution $\gamma(t)$ of the Euler-Lagrange equation (17) for any value of $n > 0$ subject to the boundary conditions

$$\left.\begin{array}{ll} \gamma(0) = a, & \gamma(T) = b \\ \frac{D\gamma(0)}{dt} = 0, & \frac{D\gamma(T)}{dt} = 0 \\ \vdots & \vdots \\ \frac{D^{2n-1}\gamma(0)}{dt^{2n-1}} = 0, & \frac{D^{2n-1}\gamma(T)}{dt^{2n-1}} = 0 \end{array}\right\} \tag{18}$$

is given by reparametrized geodesic paths between two points a and b in the Riemannian manifold, as we will show next. The solution of the Euler-Lagrange equation is derived in a coordinate-free form by making use of the following two properties of an affine connection ∇:

$$\nabla_{fX}\boldsymbol{Y} = f\nabla_X\boldsymbol{Y}, \tag{19}$$

$$\nabla_X f\boldsymbol{Y} = f\nabla_X\boldsymbol{Y} + (\mathcal{L}_X f)\boldsymbol{Y}, \tag{20}$$

where $\boldsymbol{X},\boldsymbol{Y}$ are arbitrary vector fields and f denotes a function. $\mathcal{L}$ is the Lie-derivative operator. For the solution, we make the ansatz $\gamma(t) = \gamma(\sigma(t))$ and obtain with the chain rule

$$\begin{aligned} \frac{D\boldsymbol{V}}{dt} &\equiv \nabla_{\dot\gamma(t)}\dot\gamma(t) = \nabla_{[\dot\sigma\gamma'(\sigma)]}[\dot\sigma\gamma'(\sigma)] \\ &\overset{(19)}{=} \dot\sigma\nabla_{\gamma'(\sigma)}[\dot\sigma\gamma'(\sigma)] \\ &\overset{(20)}{=} \dot\sigma^2\nabla_{\gamma'(\sigma)}\gamma'(\sigma) + \dot\sigma(\mathcal{L}_{\gamma'(\sigma)}\dot\sigma)\gamma'(\sigma) \\ &= \dot\sigma^2\nabla_{\gamma'(\sigma)}\gamma'(\sigma) + \ddot\sigma\gamma'(\sigma), \end{aligned} \tag{21}$$

where we have used $\mathcal{L}_{\gamma'(\sigma)}f = \frac{d}{d\sigma}f$ and a prime denotes differentiation with respect to arc length σ. Along a geodesic path, the geodesic equation is obeyed:

$$\frac{D\gamma'(\sigma)}{d\sigma} \equiv \nabla_{\gamma'(\sigma)}\gamma'(\sigma) = 0, \tag{22}$$

and, thus, Eq. (21) becomes $\frac{D\boldsymbol{V}}{dt} = \ddot\sigma\gamma'(\sigma)$. Similarly, we get for the k-fold covariant derivative along a geodesic path

$$\frac{D^k\boldsymbol{V}}{dt^k} = \frac{d^{k+1}\sigma(t)}{dt^{k+1}}\gamma'(\sigma), \quad k = 0,1,2,\ldots. \tag{23}$$

Inserting (23) into the Euler-Lagrange equation (17) yields, with $R(\gamma'(\sigma),\gamma'(\sigma))\gamma'(\sigma) = 0$,

$$\frac{d^{2n}\sigma(t)}{dt^{2n}} = 0, \quad n = 1,2\ldots. \tag{24}$$

Equations (22) and (24) are augmented by the boundary conditions (18), which separate into

$$\gamma^\mu(0) = a, \qquad \gamma^\mu(\Sigma) = b, \tag{25}$$

and

$$\left.\begin{array}{ll} \sigma(0) = 0, & \sigma(T) = \Sigma, \\ \dot\sigma(0) = 0, & \dot\sigma(T) = 0, \\ \vdots & \vdots \\ \frac{d^{2n-1}\sigma(0)}{dt^{2n-1}} = 0, & \frac{d^{2n-1}\sigma(T)}{dt^{2n-1}} = 0, \end{array}\right\}, \tag{26}$$

respectively, where Σ is the total length of the geodesic path and a and b are the initial and final point in the manifold. Equation (24) subject to (26) can be solved analytically in terms of the generalized hypergeometric function ${}_2F_1$ [27]:

$$\sigma(\vartheta) = \Sigma\frac{(2n-1)!\,\vartheta^n}{(n-1)!^2\,n}{}_2F_1(n; 1-n; n+1; \vartheta), \tag{27}$$

where $\vartheta = t/T$ denotes normalized time. In particular, we obtain,

$$\sigma(\vartheta) = \begin{cases} \Sigma\vartheta, & n = 1 \\ \Sigma(-2\vartheta^3 + 3\vartheta^2), & n = 2 \\ \Sigma(6\vartheta^5 - 15\vartheta^4 + 10\vartheta^3), & n = 3. \end{cases} \tag{28}$$

We conclude that the solution of the one-parameter family of variational problems (9) is given by the trajectory $\gamma(t) = \gamma(\sigma(t))$. Note that the optimal solution predicts the same geodesic path $\gamma(\sigma)$ for different values of n, but results according to (27) in different profiles for the kinetic energy $K \sim \dot\sigma^2$. Note further that the form of the solution implies

a decoupling of spatial movement properties (path, posture) from temporal ones (speed, kinetic energy), as has been assumed in the original formulation of the geodesic model and in other works [14]. Indeed, (22) and (24) can be regarded as the Euler-Lagrange equation of two variational problems

$$\delta J_1 = 0 \quad \text{with} \quad J_1 = \int d\sigma \tag{29}$$

and

$$\delta J_2 = 0 \quad \text{with} \quad J_2 = \int_0^T \left(\frac{d^n \sigma(t)}{dt^n} \right)^2 dt, \tag{30}$$

where J_1 and J_2 define the costs on the spatial and temporal levels of control, respectively. The assumptions of the original geodesic model ($n = 3$) are therefore captured by the single cost given by the squared-jerk functional in Riemann space (13). Note that the optimal solution of the one-parmater family of MSD cost functionals in Euclidean space (8) follows from the Riemannian result when assuming a Euclidean metric.

What is the physical meaning of geodesic paths in the configuration manifold, and why might they be an emergent property of the motor system? First, geodesic paths are the straightest and shortest paths in the configuration manifold, and second, they correspond to least-effort paths, where effort is defined as the amount of torques that are acting on the arm. To derive the latter result, it is useful to work in the coordinate basis $\boldsymbol{e}_\mu = \frac{\partial}{\partial q^\mu}$ and to analyze the dynamic equation (7) along an arbitrary predefined path $q^\mu(t) = q^\mu(\sigma(t))$. We obtain from (7)

$$M_{\mu\nu} \frac{dq^\nu}{d\sigma} \ddot{\sigma} + M_{\mu\nu} \left[\frac{D}{d\sigma} \left(\frac{dq^\nu}{d\sigma} \right) \right] \dot{\sigma}^2 = \tau_\mu. \tag{31}$$

The two terms on the left-hand side of (31) describe the tangential acceleration torques and the Coriolis and centripetal torques, respectively. Note that the origin of the latter lies in the intrinsic curvature of the path in configuration space. Along a geodesic path, the intrinsic curvature vanishes and the geodesic equation (22) is obeyed, which reads as, in the coordinates q^μ,

$$\frac{D}{d\sigma} \left(\frac{dq^\mu}{d\sigma} \right) = \frac{d^2 q^\mu}{d\sigma^2} + \Gamma^\mu_{\nu\lambda} \frac{dq^\nu}{d\sigma} \frac{dq^\lambda}{d\sigma} = 0. \tag{32}$$

The dynamic equation of motion (31) then simplifies to

$$M_{\mu\nu} \frac{dq^\nu}{d\sigma} \ddot{\sigma} = \tau_\mu \quad \text{or} \quad \ddot{\sigma} = \left\langle \boldsymbol{\tau}, \frac{d\boldsymbol{q}}{d\sigma} \right\rangle, \tag{33}$$

where we have used $\langle \frac{d\boldsymbol{q}}{d\sigma} \frac{d\boldsymbol{q}}{d\sigma} \rangle = 1$ in the second equation. Movements along geodesic paths can thus be considered least-effort paths and MSD derivative functionals in Riemannian space correspond to least-effort costs.

B. Comparison of the MJ model in Euclidean task space and Riemannian configuration space for movements between pointlike targets

In this section, we compare the predictions of the MJ model in Euclidean and Riemannian configuration space that is equipped with the kinetic energy metric between two pointlike targets in three-dimensional space. The two models lead to different predictions due to the differences in the underlying metric space. For simplicity, we assume that the initial and final arm configurations are predefined. The solution of the MJ variational problem (1) subject to the two-point boundary conditions

$$\left.\begin{aligned} \boldsymbol{x}(0) &= \boldsymbol{x}_0, & \boldsymbol{x}(T) &= \boldsymbol{x}_f \\ \dot{\boldsymbol{x}}(0) &= 0, & \dot{\boldsymbol{x}}(T) &= 0 \\ \ddot{\boldsymbol{x}}(0) &= 0, & \ddot{\boldsymbol{x}}(T) &= 0 \end{aligned}\right\} \tag{34}$$

is a special case of the Riemannian result. It is given by reparametrized straight paths (geodesic paths of Euclidean space) $\boldsymbol{x}(t) = \boldsymbol{x}[s(t)]$ with

$$\boldsymbol{x}(s) = \boldsymbol{x}_0 + \frac{s}{S}(\boldsymbol{x}_f - \boldsymbol{x}_0), \tag{35}$$

$$s(t) = S(10\vartheta^3 - 15\vartheta^4 + 6\vartheta^5), \tag{36}$$

where $\boldsymbol{x}_0$ and $\boldsymbol{x}_f$ are the initial and final hand positions, respectively, $\vartheta = t/T$ defines normalized time, and s is the Euclidean arc length of the hand path. T is the total movement time and $S = |\boldsymbol{x}_f - \boldsymbol{x}_0|$. The MJ model results in a bell-shaped speed profile given by $v = |\dot{s}| = 15S/(8T)[4\vartheta(1-\vartheta)]^2$. For point-to-point movements in three-dimensional space, however, the MJ model does not determine all DOF. Based on our analysis of possible coordinate sets, one may extend the hand coordinates $\boldsymbol{x}$ by the swivel angle α and formulate the MJ model for this extended set of coordinates $\hat{\boldsymbol{x}} = (\boldsymbol{x}, \alpha)$. Equation (35) is then complemented by

$$\alpha(s) = \alpha_0 + \frac{s}{S}(\alpha_f - \alpha_0), \tag{37}$$

which together define the arm configuration completely.

In contrast, the predictions of the MJ model in Riemannian space (13) are derived as follows: for given initial and final arm configurations q_a^μ and q_b^μ, respectively, we first solve the geodesic equation (32), resulting in the geodesic path $q^\mu(\sigma)$ that defines the spatial properties of the movement (see Appendices A and B for details). The temporal properties are given by (28) for $n = 3$ and the movement trajectory then follows as $q^\mu(t) = q^\mu(\sigma(t))$. Examples of geodesic hand paths in the horizontal XY plane for a two DOF arm between a central and circularly arranged targets are shown in Fig. 2(a).

Note that the driving torques ($\boldsymbol{\tau} \sim \ddot{\sigma}$) are, according to (33), double peaked with amplitudes that depend on the inertial properties of the arm. The kinetic energy profile is bell shaped ($K \sim \dot{\sigma}^2$) and hand speed v is determined by the kinetic energy according to $v = |\dot{\boldsymbol{x}}| = |\frac{d\boldsymbol{x}}{d\sigma}| \dot{\sigma} \sim K^{1/2}$, where $\boldsymbol{x}(\sigma)$ is the hand path [Fig. 2(b)].

For a detailed comparison of the MJ model in Riemannian space with experimental data of pointing movements in three-dimensional space, we refer the reader to [13].

C. Invariance principles and Killing vector fields

In the last section, we determine the movement invariants and the constants of motion associated with the geodesic model. Generally, symmetries and conservation laws define important properties of a computational model and are of particular interest for model evaluation. We first observe

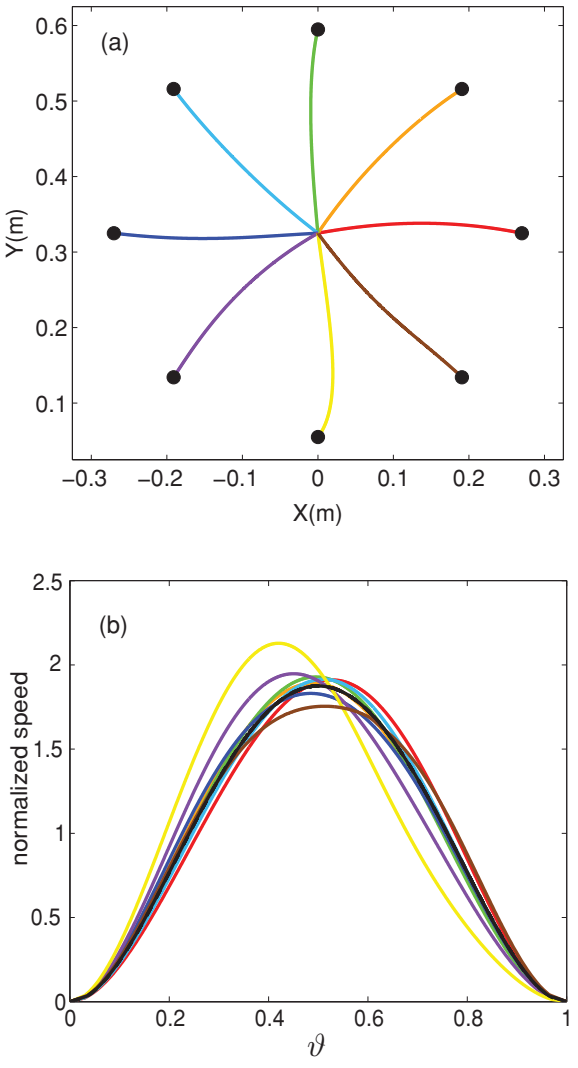

FIG. 2. (Color) (a) Geodesics paths with respect to the kinetic energy metric in the horizontal plane XY from a central initial target to circularly arranged final targets (radius: 0.27 m) in the XY plane. The shoulder joint of the arm is located at (0,0). (b) Normalized hand speed profiles along the geodesic paths of (a) as they result from the geodesic model [color code as in (a)]. $\vartheta = t/T$ is normalized time. The speed $v = |\frac{dx}{d\sigma}|\dot{\sigma}$ is normalized with respect to the average hand speed S/T, where S is the Euclidean distance between initial and final hand position and T is the total movement time. The black line shows the normalized speed profile of the original minimum-jerk model. Simulation parameters are mean values for the right arm of a male subject with total body mass $m = 85$ kg: $l_1 = 0.30$ m, $l_2 = 0.345$ m, $m_1 = 2.52$ kg, $m_2 = 2.07$ kg, $a_1 = 0.142$ m, $a_2 = 0.225$ m, $I_{1,x} = 0.019\,\mathrm{kg\,m^2}$, $I_{2,x} = 0.021\,\mathrm{kg\,m^2}$. The parameters are defined in Appendix A.

that the functional (9) scales under a change of amplitude $\boldsymbol{V}' = \omega \boldsymbol{V}$ and time $t' = \beta t$ according to $S_n' = \omega^2 \beta^{1-2n} S_n$, and, thus, the optimal solution is invariant under these transformations.

The first set of constants of motion, associated with the variational problem (9), is directly derived from the Euler-Lagrange equations (17) and is therefore independent of the specific choice of Riemannian manifold. It has been shown [31,32] that, if the trajectory satisfies the Euler-Lagrange equation (17), the following quantity is preserved:

$$I_n = \frac{(-1)^{n-1}}{2}\left\langle \frac{D^{n-1}\boldsymbol{V}}{dt^{n-1}}, \frac{D^{n-1}\boldsymbol{V}}{dt^{n-1}} \right\rangle + \sum_{j=1}^{n-1} (-1)^{(j-1)} \left\langle \frac{D^{2n-j-1}\boldsymbol{V}}{dt^{2n-j-1}}, \frac{D^{j-1}\boldsymbol{V}}{dt^{j-1}} \right\rangle. \quad (38)$$

This result follows by differentiating (38) and using the Euler-Lagrange equation (17) together with the property of the Riemannian tensor $\langle R(\boldsymbol{X},\boldsymbol{Y})\boldsymbol{Z},\boldsymbol{Z}\rangle = 0$, which holds for all vector fields $\boldsymbol{X},\boldsymbol{Y},\boldsymbol{Z}$ (in component notation this property corresponds to $R_{\lambda\lambda\mu\nu} = 0$). It is important to note that these constants of motion hold in any Riemannian manifold. For movements along geodesic paths, expression (38) simplifies to

$$I_n = \frac{(-1)^{n-1}}{2}\left(\frac{d^n\sigma}{dt^n}\right)^2 + \sum_{j=1}^{n-1}(-1)^{(j-1)}\frac{d^{2n-j}\sigma}{dt^{2n-j}}\frac{d^j\sigma}{dt^j} \quad (39)$$

and leads, for $n = 1,2,3$, to the following expressions:

$$I_1 = \tfrac{1}{2}\dot{\sigma}^2, \quad (40)$$

$$I_2 = \ddot{\sigma}\dot{\sigma} - \tfrac{1}{2}\ddot{\sigma}^2, \quad (41)$$

$$I_3 = \sigma^{(5)}\dot{\sigma} - \sigma^{(4)}\ddot{\sigma} + \tfrac{1}{2}\dddot{\sigma}^2. \quad (42)$$

The second set of constants of motion depends on the specific properties of the Riemannian manifold and is derived from Killing vector fields that describe the symmetries of the Riemannian manifold. Killing vector fields define directions in the manifold along which the metric tensor does not change and are solutions of Killing's equation [33], given by $\mathcal{L}_{\boldsymbol{\xi}} g = 0$, where $\mathcal{L}_{\boldsymbol{\xi}}$ is the Lie-derivative operator in the direction of the Killing vector field $\boldsymbol{\xi}$. In the local coordinates q^μ, where $\boldsymbol{\xi} = \xi^\mu \frac{\partial}{\partial q^\mu}$, Killing's equation can be written in the form

$$\nabla_\nu \xi_\mu + \nabla_\mu \xi_\nu = 0, \quad (43)$$

where $\nabla_\nu X_\mu = \frac{\partial X_\mu}{\partial q^\nu} - \Gamma^\lambda_{\mu\nu} X_\lambda$. In the special case where the metric tensor does not depend on one of the coordinates, say q^α, the Killing vector is given by $\boldsymbol{\xi} \equiv \frac{\partial}{\partial q^\alpha}$ with components $\xi^\mu = \delta^\mu_\alpha$. An important application of Killing vector fields lies in the following theorem: if $\boldsymbol{\xi}$ is a Killing vector and $\boldsymbol{t}$ is the tangent vector to a geodesic path, then $\langle \boldsymbol{\xi},\boldsymbol{t}\rangle$ is a constant of motion along this path. Thus, each Killing vector field induces a constant of motion along geodesic paths. Movement invariants can thus be generated by Killing vector fields. It is well known that three-dimensional Euclidean space adopts six Killing vector fields, which generate the rigid transformations (three rotations and three translations) that leave the Euclidean metric invariant. Euclidean space is maximally symmetric because it adopts the maximal possible number of Killing vectors given by $m(m+1)/2$, where m is the dimension of the manifold. In contrast, the kinetic energy metric only adopts one Killing vector field, namely, $\boldsymbol{\xi} = \frac{\partial}{\partial \eta}$ or expressed in coordinates $\xi^\mu = (0,1,0,0)$, because the kinetic energy metric is invariant under azimuthal rotations. The constant of motion induced by this Killing vector is given in local coordinates by $\langle \boldsymbol{\xi},\boldsymbol{t}\rangle = \frac{dq^\mu}{d\sigma} M_{\mu 2}$. Figure 3 shows the integral curves of the Killing vector field for movements in the XY plane of a two

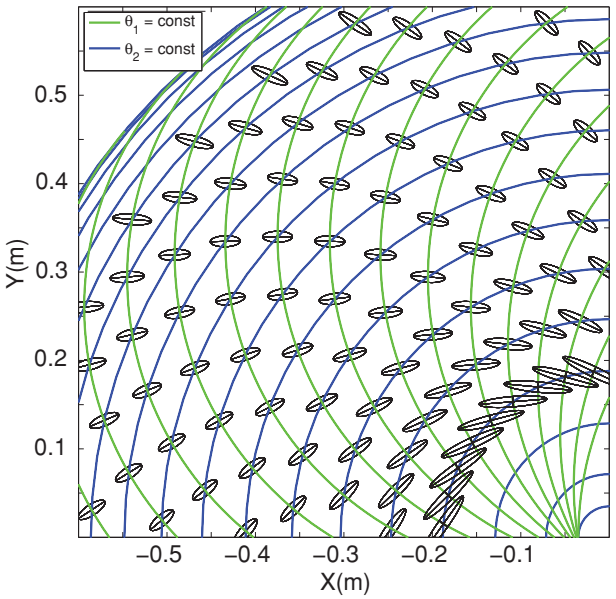

FIG. 3. (Color) Metric tensor field and Killing vector field for movements of a two DOF arm in the XY plane. The metric tensor field is shown in (x,y) coordinates and visualized by ellipses. The Killing vector field is in the directions of the coordinate lines $\theta_2 = \text{const}$ (blue solid lines). Note that the metric tensor (the size of the ellipses) along the Killing vector field does not change. The shoulder joint of the arm is located at (0,0). Simulation parameters as given in the caption of Fig. 2.

DOF arm, which correspond to the coordinate lines $\theta_2 = \text{const}$. The metric tensor field for different hand locations along the Killing vector fields is visualized by ellipses. It represents physically the effective inertial mass distribution around the hand location. Note that the metric tensor does not change along the Killing vector field.

IV. DISCUSSION

In this paper, we have provided an intrinsic formulation of human arm dynamics that is independent of the coordinate representation. We have generalized the class of kinematic MSD cost functionals from Euclidean to Riemannian space. It is important to note that MSD costs have often been suggested as important cost functions in the study of human motor control [17,27]. When applying these generalized costs to point-to-point reaching movements, we have derived their optimal solutions in terms of reparametrized geodesic paths. This result holds for any Riemannian manifold. We can then make specific choices for Riemannian manifolds and label points of the manifold in terms of specific sets of coordinates. For example, if we choose for the manifold two-dimensional Euclidean space $\mathcal{M} = \mathbb{E}^2 \equiv (\mathbb{R}^2, I)$ with Cartesian coordinates, where $I = \text{diag}(1,1)$, then Eq. (9) results in the MJ model in its original form (1). That is, the reparametrized geodesic paths in Euclidean space correspond to the well-known MJ solution in terms of straight hand paths and bell-shaped hand speed profiles.

In this paper, we have focused on the Riemannian manifold given by the arm's configuration space equipped with the kinetic energy metric $\mathcal{M} = (T^4, M_{\mu\nu})$. In this metric space, we have shown the mathematical identity of the kinematic MSD costs and their dynamical equivalents, in particular, we have deduced the equivalence of the MJ and MTC models. This result provides a new perspective with respect to a long-standing controversy of kinematic versus dynamic modeling approaches in human motor control.

Geodesic paths in the Riemannian configuration manifold have been identified as least-effort paths as well as the optimal solution of the one-parameter family of MSD costs in Riemannian space. Hence, these costs do not only maximize smoothness, but simultaneously minimize movement effort and, thus, encode two performance indices that have been suggested to play a significant role in movement optimization [34,35].

We have derived one class of movement invariants from symmetries of the underlying manifold. Whereas the MSD costs in Euclidean space are invariant to rigid transformations, the invariants of the MSD costs in Riemannian space are dictated by the local properties of a nonisotropic arm inertia. These invariants were classified in terms of Killing vector fields that define the symmetries of the metric tensor and determine constant of motions along geodesic movements.

Nevertheless, several important aspects have not been considered in this paper such as the presence of holonomic and nonholonomic constraints, the adaption to external force fields, and the effect of visual feedback.

A Riemannian geometric approach to the control of arm dynamics under constraints has been implemented in [36], where it is shown that holonomic constraints lead to a Riemannian submanifold with a naturally induced metric, whereas nonholonomic constraints result in a restricted set of tangent vectors on the original manifold. Constraints in the form of additional intermediate targets have been successfully modeled in planar obstacle-avoidance movements using the minimum-jerk model [17]. Minimization of MSD costs in a general Riemannian manifold subject to additional intermediate point constraints have been considered in [31,32].

The reaction to perturbative external force fields has been studied in [37]. In a Riemannian framework, perturbations may be analyzed in terms of geodesic deviation. Interestingly, the evolution of geodesic deviation and, thus, the stability (or instability) of the geodesic path, is determined by the curvature of the manifold [38]. On the other hand, the control of arm stiffness that stabilizes the arm against perturbing external forces can be interpreted geometrically as shaping the manifold around the movement trajectory [10,39]. It is an open question as to whether this qualitative description can be turned into a coherent mathematical model.

The availability of visual feedback from the moving hand leads to a straightening of hand paths in Euclidean space [40]. Visual feedback might be incorporated in a Riemannian framework using information geometric methods [41]. However, further studies need to demonstrate the feasibility of this approach.

In summary, we argue that the description of sensorimotor spaces and the understanding of human motor actions may benefit from a differential geometric approach that aims to

identify suitable manifolds, their symmetry transformations, and possible affine or metrical structures.

ACKNOWLEDGMENTS

A.B. was supported by the German Federal Ministry of Education and Research (BMBF) via the Bernstein Center for Computational Neuroscience (BCCN) Göttingen under Grants No. 01GQ0430 and No. 01GQ1005. A.B. thanks J.M. Hermann and F. Müller-Hoissen for helpful discussions.

APPENDIX A: FOUR DOF ARM

1. Forward and inverse kinematics

The human arm is modeled as a chain of rigid links. For the description of an arm configuration in terms of four joint angles, a parametrization as in [13] is chosen. In this representation, the elbow joint location $\boldsymbol{p} = (u,v,w)^T$ and the center of mass of the hand location $\boldsymbol{x} = (x,y,z)^T$ are determined by the joint angles $\boldsymbol{q} = (\theta,\eta,\zeta,\phi)^T$ according to

$$u = -l_1 \sin\theta \sin\eta, \quad v = l_1 \sin\theta \cos\eta, \quad w = -l_1 \cos\theta,$$

$$\begin{aligned} x &= u - l_2[(\cos\theta \sin\eta \cos\zeta + \cos\eta \sin\zeta)\sin\phi \\ &\quad + \sin\theta \sin\eta \cos\phi], \\ y &= v + l_2[(\cos\theta \cos\eta \cos\zeta - \sin\eta \sin\zeta)\sin\phi \\ &\quad + \sin\theta \cos\eta \cos\phi], \\ z &= w + l_2[\sin\theta \cos\zeta \sin\phi - \cos\theta \cos\phi], \end{aligned}$$

where l_1 and l_2 are the upper and forearm lengths, respectively. We assume in all our derivations that $|\boldsymbol{p} \times \boldsymbol{x}| \neq 0$ and $|w| < l_1$.

Another set of four generalized coordinates is defined by $\boldsymbol{q}' = (x,y,z,\alpha)^T$, which consists of the hand coordinates $\boldsymbol{x}$ and the angle α that describes the rotation of the plane spanned by the upper and forearm around the shoulder-hand axis. The rotation angle α is determined by the joint angles according to

$$\tan\alpha = \frac{l_1 \sin\theta \cos\zeta + l_2(\sin\theta \cos\zeta \cos\phi + \cos\theta \sin\phi)}{d \sin\theta \sin\zeta},$$

where $d = |\boldsymbol{x}|$ is the shoulder-hand distance. Further, we provide the relation

$$\cos\alpha = \frac{d \sin\theta \sin\zeta}{e},$$

with $e = \sqrt{x^2 + y^2}$, which will be used later for the determination of the Jacobi transformation matrix.

To derive the functional dependence of the joint angles $\boldsymbol{q}$ on the coordinates $\boldsymbol{q}'$ (inverse kinematics), we first determine the joint angles in terms of elbow and hand location. We find

$$\begin{aligned} \theta &= a\cos\left(\frac{-w}{l_1}\right), \quad \eta = a\tan2(-u,v), \\ \zeta &= a\tan2[l_1(uy - vx), v(vz - wy) - u(wx - uz)], \\ \phi &= a\cos\left(\frac{x^2 + y^2 + z^2 - l_1^2 - l_2^2}{2l_1 l_2}\right), \end{aligned}$$

where the two argument $a\tan2$ function is $a\tan2(a,b) := a\tan(\frac{a}{b}) - \text{sign}(a)[1 - \text{sign}(b)]\frac{\pi}{2}$. The inverse kinematic relations follow when combining the previous expressions with the relation that gives the elbow location as a function of hand position and the rotation angle α. All elbow positions lie on the intersection circle of two spheres that have centers at the shoulder and hand position with radii l_1 and l_2, respectively. We get

$$\boldsymbol{p}(\boldsymbol{x},\alpha) = R_z(\varphi) R_y(\vartheta)[f\boldsymbol{e}_x + r\boldsymbol{e}_r(\alpha)],$$

where the radial distance to the center of the intersection circle is $f = \frac{1}{2d}(l_1^2 - l_2^2 + d^2)$ and the intersection circle radius is $r = \frac{1}{2d}\sqrt{4d^2 l_1^2 - (l_1^2 - l_2^2 + d^2)^2}$. Furthermore, it is $\varphi = a\tan2(y,x)$, $\vartheta = a\sin(z/d)$, $\boldsymbol{e}_x = (1,0,0)^T$, and $\boldsymbol{e}_r(\alpha) = (0, -\cos\alpha, -\sin\alpha)^T$. R_y and R_z define rotation matrices around the y and z axes, respectively, and are given by

$$R_y(\vartheta) = \begin{pmatrix} \cos\vartheta & 0 & -\sin\vartheta \\ 0 & 1 & 0 \\ \sin\vartheta & 0 & \cos\vartheta \end{pmatrix}$$

and

$$R_z(\varphi) = \begin{pmatrix} \cos\varphi & -\sin\varphi & 0 \\ \sin\varphi & \cos\varphi & 0 \\ 0 & 0 & 1 \end{pmatrix}.$$

2. Jacobi transformation matrix Λ

The transformation matrix from the coordinates $q^\mu = (\theta,\eta,\zeta,\phi)$ to the coordinates $q'^\mu = (x,y,z,\alpha)$ is given by $\Lambda^\mu_\nu = \frac{\partial q'^\mu}{\partial q^\nu}$. The nonzero components are

$$\begin{aligned} \Lambda^1_1 &= -l_1 \cos\theta \sin\eta - l_2(\cos\theta \sin\eta \cos\phi \\ &\quad - \sin\theta \sin\eta \cos\zeta \sin\phi), \\ \Lambda^1_2 &= -l_1 \sin\theta \cos\eta - l_2[\cos\eta(\cos\theta \cos\zeta \sin\phi \\ &\quad + \sin\theta \cos\phi) - \sin\eta \sin\zeta \sin\phi], \\ \Lambda^1_3 &= l_2 \sin\phi(\cos\theta \sin\eta \sin\zeta - \cos\eta \cos\zeta), \\ \Lambda^1_4 &= l_2[\sin\theta \sin\eta \sin\phi - \cos\phi(\cos\theta \cos\zeta \sin\eta \\ &\quad + \cos\eta \sin\zeta)], \end{aligned}$$

$$\begin{aligned} \Lambda^2_1 &= l_1 \cos\theta \cos\eta + l_2 \cos\eta(\cos\theta \cos\phi \\ &\quad - \sin\theta \cos\zeta \sin\phi), \\ \Lambda^2_2 &= -l_1 \sin\theta \sin\eta - l_2[\sin\eta(\cos\theta \cos\zeta \sin\phi + \sin\theta \cos\phi) \\ &\quad + \cos\eta \sin\zeta \sin\phi], \\ \Lambda^2_3 &= -l_2 \sin\phi(\sin\eta \cos\zeta + \cos\theta \cos\eta \sin\zeta), \\ \Lambda^2_4 &= l_2[\cos\eta(\cos\theta \cos\zeta \cos\phi - \sin\theta \sin\phi) \\ &\quad - \sin\eta \sin\zeta \cos\phi], \end{aligned}$$

$$\begin{aligned} \Lambda^3_1 &= l_1 \sin\theta + l_2(\cos\theta \cos\zeta \sin\phi + \sin\theta \cos\phi), \\ \Lambda^3_3 &= -l_2 \sin\theta \sin\zeta \sin\phi, \\ \Lambda^3_4 &= l_2(\cos\theta \sin\phi + \sin\theta \cos\zeta \cos\phi), \end{aligned}$$

$$\Lambda_1^4 = -\frac{d}{e^2} l_2 \sin\zeta \sin\phi,$$

$$\Lambda_3^4 = -\frac{d}{e^2}[l_1 \sin^2\theta + l_2 \sin\theta(\sin\theta\cos\phi + \cos\theta\cos\zeta\sin\phi)],$$

$$\Lambda_4^4 = \frac{l_2 \sin\theta \sin\zeta}{2de^2}\big[2l_2^2(\cos\theta\cos\phi - \sin\theta\cos\zeta\sin\phi) + l_1 l_2(3\cos\theta + \cos\theta\cos 2\phi - \sin\theta\cos\zeta\sin 2\phi) + 2l_1^2\cos\theta\cos\phi\big],$$

where we have used the identity

$$\Lambda_\nu^4 = \frac{\partial\alpha}{\partial q^\nu} = \frac{\partial \arctan(\tan\alpha)}{\partial q^\nu} = \frac{1}{1+\tan^2\alpha}\frac{\partial\tan\alpha}{\partial q^\nu} = \cos^2\alpha\frac{\partial\tan\alpha}{\partial q^\nu}.$$

3. Kinetic energy metric

The kinetic energy in the local coordinates $q^\mu = (\theta,\eta,\zeta,\phi)$ is given by

$$K = \tfrac{1}{2} M_{\mu\nu}(q)\dot{q}^\mu\dot{q}^\nu,$$

where the nonzero components of the kinetic energy metric $M_{\mu\nu}$ are

$$\begin{aligned}
M_{11} &= I_1 + 2I_5\cos\phi + I_3\cos^2\zeta + I_3\sin^2\zeta\cos^2\phi + I_4\sin^2\zeta\sin^2\phi,\\
M_{12} &= -\{[I_5 + (I_3 - I_4)\cos\phi]\cos\theta + (-I_3 + I_4)\sin\theta\cos\zeta\sin\phi\}\ \sin\zeta\sin\phi,\\
M_{13} &= -[I_5 + (I_3 - I_4)\cos\phi]\sin\zeta\sin\phi,\\
M_{14} &= (I_3 + I_5\cos\phi)\cos\zeta,\\
M_{22} &= I_1\sin^2\theta + (I_2 + I_3\sin^2\phi)\cos^2\theta + I_4\sin^2\theta\cos^2\zeta\sin^2\phi + (I_4\cos^2\theta + I_3\sin^2\theta\cos^2\zeta)\cos^2\phi + I_5\sin 2\theta\cos\zeta\sin\phi + [2I_5\sin^2\theta + (I_3 - I_4)\sin 2\theta\cos\zeta\sin\phi]\cos\phi + I_3\sin^2\theta\sin^2\zeta,\\
M_{23} &= (I_2 + I_4\cos^2\phi + I_3\sin^2\phi)\cos\theta + [I_5 + (I_3 - I_4)\cos\phi]\sin\theta\cos\zeta\sin\phi,\\
M_{24} &= (I_3 + I_5\cos\phi)\sin\theta\sin\zeta,\\
M_{33} &= I_2 + I_4\cos^2\phi + I_3\sin^2\phi,\\
M_{44} &= I_3,
\end{aligned}$$

with $M_{\mu\nu} = M_{\nu\mu}$ and constants

$$I_1 = I_{1,x} + m_1 a_1^2 + m_2 l_1^2, \quad I_2 = I_{1,z},$$
$$I_3 = I_{2,x} + m_2 a_2^2, \quad I_4 = I_{2,z}, \quad I_5 = m_2 l_1 a_2.$$

The parameters m_i, l_i, a_i $(i = 1,2)$, denote mass, length, and distance to the center of mass of the upper and forearm, respectively. The principal moments of inertia around the transversal (x,y) and longitudinal (z) axes of the limbs at the center of mass are denoted by $I_{i,x}$, $I_{i,y}$, $I_{i,z}$ $(i = 1,2)$. It is assumed that the transversal components of the moment of inertia for the upper arm and forearm, respectively, are the same, i.e., $I_{1,x} = I_{1,y}$ and $I_{2,x} = I_{2,y}$.

The Christoffel symbols of the second kind follow from the metric according to

$$\Gamma_{\mu\nu}^\lambda = M^{\lambda\rho}\left(\frac{\partial M_{\mu\rho}}{\partial x^\nu} + \frac{\partial M_{\nu\rho}}{\partial x^\mu} - \frac{\partial M_{\mu\nu}}{\partial x^\rho}\right),$$

and can be computed explicitly by using symbolic mathematics software packages such as MATHEMATICA or MAPLE.

4. Geodesic paths

The determination of the geodesic path in the configuration manifold follows from the solution of the geodesic equation. The geodesic equation for a four DOF arm can be written as a system of eight first-order ordinary differential equations (ODEs) by setting $y_1 = \theta$, $y_2 = \eta$, $y_3 = \zeta$, $y_4 = \phi$, $y_5 = \dot{\theta}$, $y_6 = \dot{\eta}$, $y_7 = \dot{\zeta}$, and $y_8 = \dot{\phi}$, leading to (a dot denotes here differentiation with respect to the path parameter λ)

$$\dot{y}_1 = y_5, \quad \dot{y}_2 = y_6, \quad \dot{y}_3 = y_7, \quad \dot{y}_4 = y_8, \quad \dot{y}_5 = -\Gamma_{ij}^1 u^i u^j,$$
$$\dot{y}_6 = -\Gamma_{ij}^2 u^i u^j, \quad \dot{y}_7 = -\Gamma_{ij}^3 u^i u^j, \quad \dot{y}_8 = -\Gamma_{ij}^4 u^i u^j,$$

where we have defined $u^i = y_{i+4}$ $(i = 1,2,3,4)$. The system of ODEs subject to the boundary conditions $y_1(0) = \theta(0)$, $y_2(0) = \eta(0)$, $y_3(0) = \zeta(0)$, $y_4(0) = \phi(0)$, $y_1(1) = \theta(1)$, $y_2(1) = \eta(1)$, $y_3(1) = \zeta(1)$, and $y_4(1) = \phi(1)$ defines a two-point boundary value problem, which can be solved numerically by using shooting methods (e.g., MATLAB, bvp4c), [42]. One remark about the parametrization of the geodesic path is needed. The geodesic path as it results from the solution of the system of ODEs is parametrized with respect to an arbitrary parameter $\lambda \in [0,1]$. However, the parameter λ defines automatically an affine parameter because it is proportional to the Riemannian arc length σ. The parameters are related by $\lambda = \sigma/\Sigma$, where the total length of the geodesic path Σ follows from

$$\Sigma = \int_0^1 \sqrt{M_{\mu\nu}\frac{dq^\mu}{d\lambda}\frac{dq^\nu}{d\lambda}}\,d\lambda$$

and $q^\mu(\lambda)$ defines the geodesic path.

The reparameterization of the geodesic path in terms of the parameter σ can thus be easily performed.

APPENDIX B: TWO DOF ARM

1. Forward and inverse kinematics

For the special case where the arm moves in the XY plane of the shoulder-centered frame (Fig. 1), the joint angle coordinates have the form $q^\mu = (\pi/2, \theta_1 - \pi/2, \pi/2, \theta_2)$, where θ_1 is the angle enclosed by the upper arm and the X axis and θ_2 is the flexion angle. It is convenient for the following to define the two-dimensional joint angle coordinates $h^\mu = (\theta_1, \theta_2)$ and the hand position coordinates $h'^\mu = (x,y)$. The coordinates are related according to

$$x = l_1\cos\theta_1 + l_2\cos(\theta_1 + \theta_2),$$
$$y = l_1\sin\theta_1 + l_2\sin(\theta_1 + \theta_2),$$

and

$$\theta_1 = a\tan2(y,x) - a\cos\left(\frac{d^2 + l_1^2 - l_2^2}{2l_1 d}\right),$$
$$\theta_2 = \pi - a\cos\left(\frac{l_1^2 + l_2^2 - d^2}{2l_1 l_2}\right)$$

with $d = \sqrt{x^2 + y^2}$.

2. Jacobi transformation matrix Λ

The Jacobi transformation matrix Λ is given by $\Lambda^{\mu}_{\nu} = \frac{\partial h'^{\mu}}{\partial h^{\nu}}$ with components

$$\Lambda^1_1 = -l_1 \sin\theta_1 - l_2 \sin(\theta_1 + \theta_2),$$
$$\Lambda^1_2 = -l_2 \sin(\theta_1 + \theta_2),$$
$$\Lambda^2_1 = l_1 \cos\theta_1 + l_2 \cos(\theta_1 + \theta_2),$$
$$\Lambda^2_2 = l_2 \cos(\theta_1 + \theta_2).$$

3. Kinetic energy metric

The kinetic energy in the coordinates $h^{\mu} = (\theta_1, \theta_2)$ is

$$K = \tfrac{1}{2} M_{\mu\nu}(h)\dot{h}^{\mu}\dot{h}^{\nu},$$

where

$$M_{11} = I_1 + I_3 + 2I_5 \cos\theta_2,$$
$$M_{12} = I_3 + I_5 \cos\theta_2,$$
$$M_{22} = I_3.$$

Note that the components of the metric tensor do not depend on θ_1.

The Christoffel symbols of the second kind then follow as

$$\Gamma^1_{11} = -\frac{I_5(I_3 + I_5\cos\theta_2)\sin\theta_2}{I_1 I_3 - I_5^2 \cos^2\theta_2},$$
$$\Gamma^1_{12} = -\frac{I_3 I_5 \sin\theta_2}{I_1 I_3 - I_5^2 \cos^2\theta_2},$$
$$\Gamma^1_{22} = -\frac{I_3 I_5 \sin\theta_2}{I_1 I_3 - I_5^2 \cos^2\theta_2},$$
$$\Gamma^2_{11} = \frac{I_5(I_1 + I_3 + 2I_5\cos\theta_2)\sin\theta_2}{I_1 I_3 - I_5^2 \cos^2\theta_2},$$
$$\Gamma^2_{12} = \frac{I_5(I_3 + I_5\cos\theta_2)\sin\theta_2}{I_1 I_3 - I_5^2 \cos^2\theta_2},$$
$$\Gamma^2_{22} = \frac{I_5(I_3 + I_5\cos\theta_2)\sin\theta_2}{I_1 I_3 - I_5^2 \cos^2\theta_2},$$

with $\Gamma^{\lambda}_{\mu\nu} = \Gamma^{\lambda}_{\nu\mu}$. We remark that any two-dimensional Riemannian manifold is conformally flat, i.e., there exist new coordinates $\tilde{h}^{\mu} = (u,v)$ for which the line element takes the form $d\sigma^2 = \Omega^2(u,v)(du^2 + dv^2)$, where Ω^2 is the conformal factor. The metric tensor thus has Euclidean form up to a global, position-dependent stretch factor. The new coordinates are related to the old ones as

$$u = \frac{1}{\sqrt{2}}\left(\theta_1 + \int^{\theta_2} \frac{M_{12}(w) - \sqrt{|M(w)|}}{M_{11}(w)} dw\right),$$
$$v = \frac{1}{\sqrt{2}}\left(\theta_1 + \int^{\theta_2} \frac{M_{12}(w) + \sqrt{|M(w)|}}{M_{11}(w)} dw\right),$$

where $|M| = \det(M_{\mu\nu})$ and $\Omega^2 = M_{11}$.

The integrations in the expressions for u and v can be performed, but lead to elliptical integrals. Although the metric tensor has diagonal form in the new coordinates, the computation of the geodesic paths is thereby not much simplified because, for this purpose, the conformal factor Ω^2 must be expressed in the new coordinates (u,v).

4. Geodesic paths

The geodesic equation for a two DOF arm can be written as a system of four first-order ODEs by setting $y_1 = \theta_1$, $y_2 = \theta_2$, $y_3 = \dot{\theta}_1$, and $y_4 = \dot{\theta}_2$, leading to

$$\dot{y}_1 = y_3, \quad \dot{y}_2 = y_4,$$
$$\dot{y}_3 = -\left(\Gamma^1_{11} y_3^2 + 2\Gamma^1_{12} y_3 y_4 + \Gamma^1_{22} y_4^2\right),$$
$$\dot{y}_4 = -\left(\Gamma^2_{11} y_3^2 + 2\Gamma^2_{12} y_3 y_4 + \Gamma^2_{22} y_4^2\right)$$

with boundary conditions $y_1(0) = \theta_1(0)$, $y_2(0) = \theta_2(0)$, $y_1(1) = \theta_1(1)$, and $y_2(1) = \theta_2(1)$.

[1] A. Pellionisz and R. Llinás, Neuroscience (Amsterdam, Neth.) **5**, 1125 (1980).
[2] M. Arbib and S. Amari, J. Theor. Biol. **112**, 123 (1985).
[3] E. Mach, *Space and Geometry: In the Light of Physiological, Psychological and Physical Inquiry* (Dover Publications Inc., NY, 2004).
[4] H. Poincaré, *Science and Hypothesis* (Dover Publications Inc., NY, 1952).
[5] R. K. Luneburg, *Mathematical Analysis of Binocular Vision* (Princeton University Press, Princeton, NJ, 1947).
[6] J. Koenderink, A. van Doorn, and J. Lappin, Perception **29**, 69 (2000).
[7] J. Todd, A. Oomes, J. J. Koenderink, and A. Kappers, Psychol. Sci. **12**, 191 (2001).
[8] J. Todd and J. Norman, Percept. Psychophys. **65**, 37 (2003).
[9] D. Hestenes, Neural Networks **7**, 65 (1994).
[10] D. Hestenes, Neural Networks **7**, 79 (1994).
[11] T. Flash and A. Handzel, Biol. Cybern. **96**, 577 (2007).
[12] M. Žefran, V. Kumar, and C. Croke, IEEE Trans. Robot. Autom. **14**, 576 (1998).
[13] A. Biess, D. Liebermann, and T. Flash, J. Neurosci. **27**, 13045 (2007).
[14] E. Torres and R. Andersen, J. Neurophysiol. **88**, 2355 (2002).
[15] E. Fasse, N. Hogan, B. Kay, and F. Mussa Ivaldi, Biol. Cybern. **82**, 69 (2000).
[16] A. Polpitiya, W. Dayawansa, C. Martin, and B. Ghosh, IEEE Trans. Autom. Control **52**, 170 (2007).
[17] T. Flash and N. Hogan, J. Neurosci. **5**, 1688 (1985).
[18] Y. Uno, M. Kawato, and R. Suzuki, Biol. Cybern. **61**, 89 (1989).
[19] E. Nakano, H. Imamizu, R. Osu, Y. Uno, H. Gomi, T. Yoshioka, and M. Kawato, J. Neurophysiol. **81**, 2140 (1999).

[20] C. Harris and D. Wolpert, Nature (London) **394**, 780 (1998).
[21] E. Todorov and J. Jordan, Nat. Neurosci. **5**, 1226 (2002).
[22] E. Todorov, Nat. Neurosci. **7**, 907 (2004).
[23] R. Murray, Z. Li, and S. S. Sastry, *A Mathematical Introduction to Robotic Manipulation* (CRC Press, Boca Raton, Florida, 1994).
[24] J. L. Synge, Philos. Trans. R. Soc. London, Ser. A **226**, 31 (1927).
[25] T. Kang, J. He, and S. I. H. Tillery, Exp. Brain Res. **167**, 352 (2005).
[26] C. G. Atkeson and J. M. Hollerbach, J. Neurosci. **5**, 2318 (1985).
[27] M. J. E. Richardson and T. Flash, J. Neurosci. **22**, 8201 (2002).
[28] S. Ben Itzhak and A. Karniel, Neural Computation **20**, 779 (2008).
[29] M. do Carmo, *Riemannian Geometry* (Birkhuser, Boston, 1992).
[30] M. Camarinha and F. Leite, IMA J. Math. Control Inf. **12**, 399 (1995).
[31] H. Popiel, Math. Control Signals Syst. **19**, 235 (2007).
[32] H. Machado, F. S. Leite, and K. Krakowski, J. Dynam Control Syst **16**, 121 (2010).
[33] M. Nakahara, *Geometry, Topology and Physics* (IOP Publishing Ltd, Bristol, UK, 1990).
[34] B. Berret, C. Darlot, F. Jean, T. Pozzo, C. Papaxanthis, and J. Gauthier, PLoS Comput. Biol. **4**, e1000194 (2008).
[35] E. Guigon, P. Baraduc, and M. Desmurget, J. Neurophysiol. **97**, 331 (2007).
[36] S. Arimoto, M. Yoshida, M. Sekimoto, and K. Tahara, J. Robotics **2009**, 1 (2009).
[37] R. Shadmehr and F. A. Mussa-Ivaldi, J. Neurosci. **14**, 3208 (1994).
[38] L. Casetti, M. Pettini, and E. Cohen, Phys. Rep. **337**, 237 (2000).
[39] N. Hogan, J. Dyn. Syst.-T ASME **107**, 1 (1985).
[40] D. Wolpert, Z. Ghahramani, and M. Jordan, Exp. Brain Res. **98**, 153 (1994).
[41] S. Amari and H. Nagaoka, *Methods of Information Geometry* (American Mathematical Society, Providence, 2000).
[42] A. Biess, M. Nagurka, and T. Flash, Bio. Cybern. **95**, 31 (2006).